Asociación Argentina
de Mecánica Computacional

Mecánica Computacional Vol XXIX, págs. 4325-4340 (artículo completo)
Eduardo Dvorkin, Marcela Goldschmit, Mario Storti (Eds.)
Buenos Aires, Argentina, 15-18 Noviembre 2010

DETERMINATION OF A SECANT MODULUS FROM MATERIAL TESTS FOR THE EFFICIENT SIMULATION OF POLYETHYLENE PIPES IN RINGSTIFFNESS TESTS

Fabian Fuerle and Johann Sienz

Civil and Computational Engineering Centre, Swansea University, Swansea, UK,
J.Sienz@swansea.ac.uk, http://www.swan.ac.uk

Keywords: Polyethylene pipes, material testing, simulation, ringstiffness test.

Abstract. Pipes made from high density polyethylene subject to the Ringstiffness test to BS EN 1446: 1996 are sought to be simulated by means of the Finite Element Method. Companies often express their interest in simple and very efficient calculations providing results almost instantly. Thus a linear elastic material model will be employed even though for good accuracy the simulation of a visco-elastic material would require a time dependent model. To improve the accuracy of the simulations material tests are conducted and a guideline is developed to extract a secant modulus that takes temperature, strain rate and strain level into account.

1 INTRODUCTION

An accurate simulation of polyethylene pipes subject to the Ringstiffness test to BS EN 1446: 1996 (see Figure 1, Figure 2 and (British Standards Institution, 1996)) requires a time dependent material model. Usage of such a model naturally leads to higher computational effort. Especially companies express their interest in simple and very efficient calculations providing results almost instantly. At the same time the desired degree of accuracy often allows for the use of a more simplified approach. Furthermore, usually the final state of the pipe is of interest rather than the entire history. Thus a linear elastic material model is both desirable and applicable.

Figure 1: Pipe samples placed in stiffness machine.

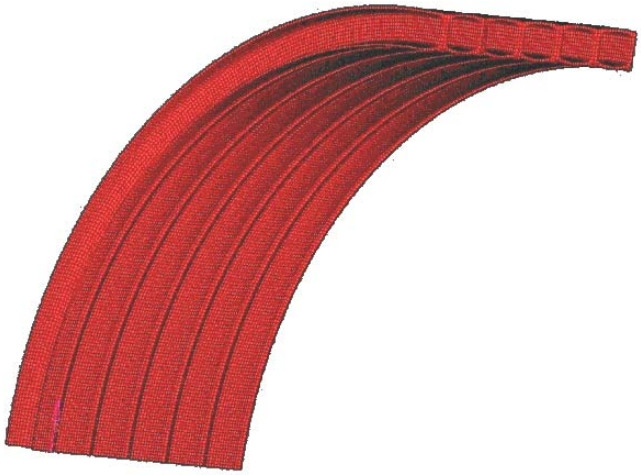

Figure 2: Typical FE model simulating the Ringstiffness test.

Material tests for high density polyethylene (HDPE), in particular Dynamic Mechanical Thermal Analyses (DMTA), have been conducted by (Sha et al. 1991; Love et al. 2005). Regarding the former work the frequencies the tests were conducted with are too high for the data to be applicable to the Ringstiffness tests and the latter focuses on blends of polyethylene and reactive terpolymer blends. (Bilgin et al. 2007) give an estimate for a secant modulus that takes the temperature into account but assumes a certain strain rate and strain level. Modeling of polyethylene pipes subject to the Ringstiffness tests is discussed by (Moore and Zhang, 1998). The former article discusses a linear and the latter a non-linear visco-elastic material model.

For the sake of simplicity and efficiency the present work is aiming at maximizing the degree of accuracy while using a linear elastic approach. Thus the purpose of the present work is obtaining data from material tests and providing a guideline how to extract an equivalent secant modulus, depending on the input parameters temperature, strain rate and strain level. With regards to the temperature, one can assume that a pipe that is stored in a location of constant ambient temperature has no variation across its volume. Therefore no error is made if material properties are used for one specific temperature. Uniformity in that sense naturally cannot be assumed for the strain field. That means both, the strain level and the strain rate, cannot be respected in a satisfying way with a single set of material properties for the entire pipe. But because of the fact that inexpensive simulations are sought for this inaccuracy will

be accepted as long as it is within reasonable limits.

One way to reduce the error made by utilizing a linear material model is to calculate a mean strain level and, with the pipe's deformation speed at hand, a mean strain rate. With those values, corresponding material properties can be obtained.

For a linear elastic isotropic material model two material properties are required. These are the E-modulus and the Poisson's ratio. The dependence upon the temperature, strain level and the strain rate of the E-modulus is going to be investigated. The Poisson's ratio will be taken as described in (Bilgin et al. 2007) being dependent only upon the temperature.

In order to investigate the material's stiffness several material tests of two different types will be conducted. These are DMTA and tension tests.

This paper is structured as follows: First the DMTA is introduced, the theoretical background is given and its application is described. After that the same information is given for the tension test. Subsequently a guideline for the extraction of a secant modulus for the use in a linear elastic material model is presented, followed by some examples.

2 DYNAMIC MECHANICAL THERMAL ANALYSIS

2.1 Introduction

In a DMTA test a specimen is typically tested by applying an oscillating force or displacement, while passing through a specified temperature interval. Furthermore within one test, the oscillation frequency can take several values. This testing procedure is a convenient way to investigate the material stiffness at various temperatures, while analyzing the visco-elastic behaviour at the same time, by utilizing different frequencies.

2.2 Theory

2.2.1 Strain Level and Strain Rate

Within this study the DMTA specimens are tested in a three point bending test, where all three supports are fully clamped. A typical specimen can be seen in Figure 3.

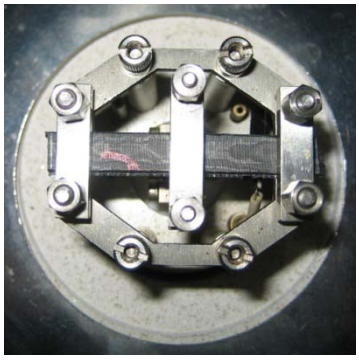

Figure 3: Specimen in clamped three point bending device of the DMTA machine. The middle support is subjected to an oscillating displacement.

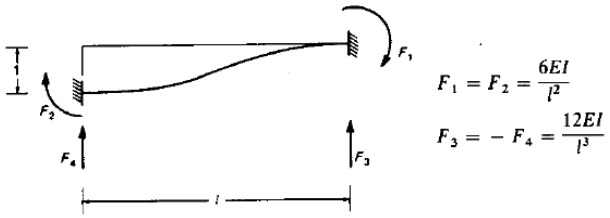

Figure 4: Theoretical moments and forces at the supports of the clamped bending test.

As illustrated in Figure 4 the theoretical moment at the supports of a clamped beam with a flexural rigidity EI and a length l equals to

$$M_{support} = \frac{6 \cdot EI \cdot d}{l^2} \tag{1}$$

if one of the supports is displaced by d. Due to the linearity of the bending moment its function along the beam axis x is

$$M(x) = \frac{6 \cdot EI \cdot d}{l^2} \cdot \left(1 - 2\frac{x}{l}\right) \quad \text{with} \quad 0 \leq x \leq l \tag{2}$$

The bending strain is

$$\varepsilon(x,y) = M(x) \cdot \frac{y}{EI} \tag{3}$$

where y is the vertical distance from the center of gravity to the location of the desired strain. Inserting Eq. 2 into Eq. 3 yields

$$\varepsilon(x,y) = \frac{6 \cdot d \cdot y}{l^2} \cdot \left(1 - 2\frac{x}{l}\right) \tag{4}$$

In order to obtain an average strain $\bar{\varepsilon}$, the strain function in Eq. 4 is integrated along half the beam and from the centre of gravity of the cross-section to the extreme fiber at the top. This integral is divided by the product of half the length and half the height.

$$\bar{\varepsilon} = \int_0^{y_{max}} \int_0^{l/2} \varepsilon(x,y)\, dx\, dy \cdot \frac{1}{l/2 \cdot y_{max}} = \frac{6 \cdot d \cdot y_{max}}{l^2} \tag{5}$$

In Figure 5 the qualitative displacement of a specimen in a typical DMTA test is plotted against time.

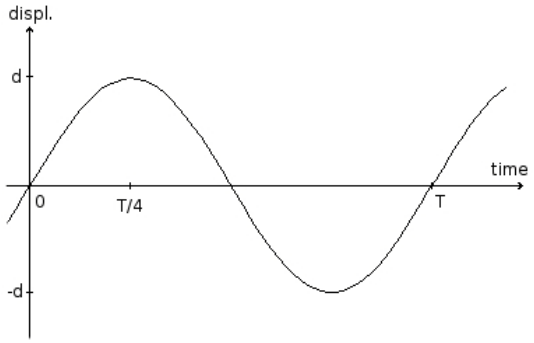

Figure 5: Displacement of the specimen in DMTA test plotted against time.

The average strain rate $\dot{\bar{\varepsilon}}$ is idealized as the average strain $\bar{\varepsilon}$ divided by a quarter of the period T, which is the strain amplitude divided by the time required to reach it starting from zero strain.

$$\dot{\bar{\varepsilon}} = \frac{\bar{\varepsilon}}{T/4} = 4 \cdot \bar{\varepsilon} \cdot f \tag{6}$$

where f is the frequency of the oscillating displacement.

2.2.2 Output

Further information on the following discussion can be found in (Hall, 1989; Ferry, 1980). The induced strain in a DMTA test is sinusoidal and reads for amplitude ε_0 and frequency f:

$$\varepsilon = \varepsilon_0 \cdot \sin(f \cdot t) \tag{7}$$

Due to the visco-elasticity of the material the induced strain and the measured stress are out of phase by an angle δ because the material does not react instantly but with a certain time lag. The stress reads:

$$\sigma = \sigma_0 \cdot \sin(f \cdot t + \delta) \tag{8}$$

The stress can be decomposed into

$$\sigma = \sigma_0 \cdot \sin(f \cdot t) + \sigma_0 \cdot \cos(f \cdot t) \cdot \sin(\delta) \tag{9}$$

Stress, strain and out-of-phase angle are illustrated in Figure 6 for two different frequencies.

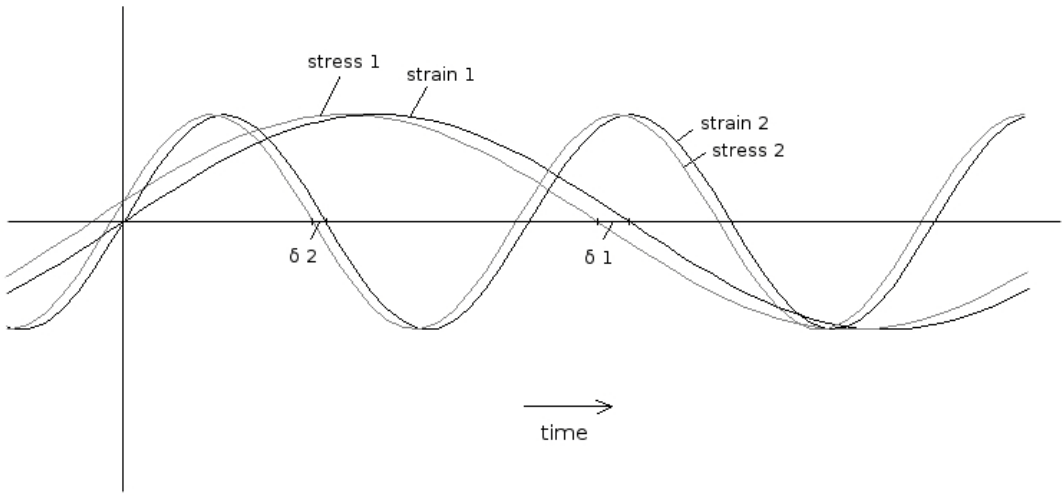

Figure 6: Illustration of dynamic stress, strain and out-of-phase angle δ for two different frequencies with $f1 > f2$.

Now, the stress is divided into an in-phase part and one that is shifted by 90°, denoting the former elastic and the latter viscous stress. With that distinction the storage and loss moduli are defined as

$$E' = \frac{\sigma_0}{\varepsilon_0}\cos(\delta) \tag{10}$$

$$E'' = \frac{\sigma_0}{\varepsilon_0}\sin(\delta) \tag{11}$$

The relation between the two moduli defines the loss tangent *tan δ*.

$$\tan(\delta) = \frac{E''}{E'} \tag{12}$$

The DMTA tests output two material properties. The storage modulus *E'* and the loss

tangent *tan δ*.

2.3 Conducted Tests and Results

Four tests were conducted at frequencies 3, 1, 0.3, 0.1, 0.03 and 0.02 Hz. Each test was carried out with a temperature between -5 ºC and 90 ºC, which changed at a rate of 1 ºC/min. The samples are 7 mm wide and 2.4 mm thick. Each of the two spans of the three point bending is 14 mm long. The middle support's maximum deformation was set to 20µm in either direction.

Inserting the deformation of the support $d=0.02mm$, the length of the beam $l=14mm$ and the location of the extreme fiber $y_{max}=1.2mm$ into Eq. 5 yields the average strain level

$$\bar{\varepsilon} = 1.83674 \cdot 10^{-4} \tag{13}$$

Insertion of Eq. 13 into Eq. 6 produces the average strain rate, naturally dependent upon the frequency

$$\dot{\bar{\varepsilon}} = 7.34694 \cdot 10^{-4} \cdot f \tag{14}$$

All obtained curves have been fitted by polynomials and all curves for the same frequency were averaged. The fitted and averaged storage moduli for the changing temperatures and frequencies are shown in Figure 7.

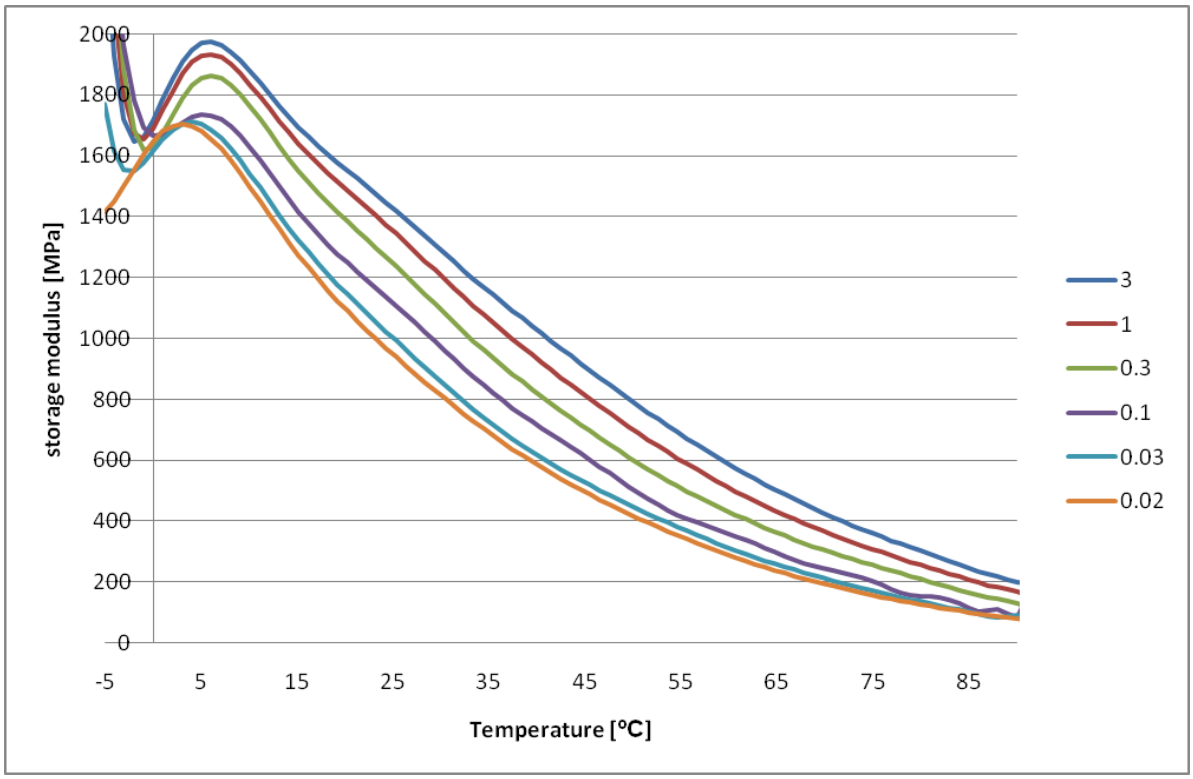

Figure 7: Storage modulus E' plotted against temperature for various frequencies obtained from DMTA tests.

Note that at the beginning of the test that means for low temperatures the DMTA machine requires some time to take the first reading. This especially applies to lower frequencies because, due to the long period, one reading takes longer than for higher ones. Therefore in that range the fitted curves are based on no or scattered data. For 0.02 and 0.03 Hz the data

becomes accurate for temperatures higher than 3°C. For the loss tangent another problem occurs for high temperatures. Here data is available but becomes very inaccurate and noisy. For the two frequencies in question the loss tangents should only be considered up to a temperature of about 45°C. One can see the decrease in material stiffness with increasing temperature and decreasing frequency. For instance for a frequency of 0.3Hz the storage modulus drops from 1988 MPa at 0°C to 195 MPa at 90°C.

The loss tangents for the temperature range and various frequencies are shown in Figure 8.

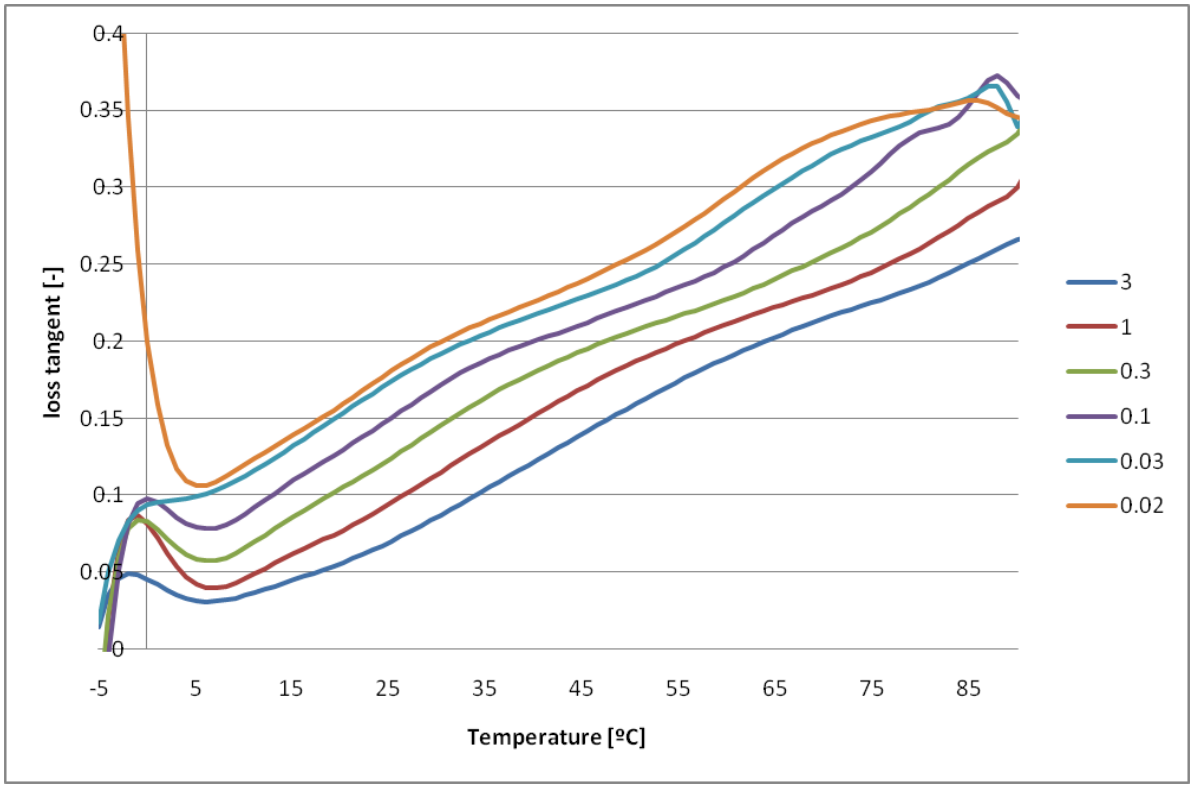

Figure 8: Loss tangent tan δ plotted against temperature for various frequencies obtained from DMTA tests.

The behaviour of the loss tangent is obviously oppositional to that of the storage modulus. It increases with increasing temperature and decreasing frequency. For a frequency of 0.3Hz the loss tangent increases from 0.055 at 0°C to 0.324 at 90°C. Since *tan δ* is an indicator for the degree of the visco-elastic effect, with *tan δ=0* being purely elastic, it is not surprising that it increases with increasing temperature. But it is surprising that it decreases with increasing frequency because one would expect that, similar to an ideal damper, the damping effect becomes more significant with higher deformation speeds. The explanation for that contradiction can be found by studying Figure 6. The two out-of-phase angles are of similar size thus the DMTA machine would output identical loss tangents for both tests even though the angle for the higher frequency is higher in relation to its period. That means the loss tangent has to be set into relation to its frequency for it to represent the degree of the visco-elastic effect. In reality the effect naturally increases with increasing frequency. This will be shown when the results of the tension tests are investigated in Section 3.3.1.

3 TENSION TESTS

3.1 Introduction

Contrary to the DMTA tests, tension tests have a constant temperature and a constant strain rate throughout one test, but they allow for the investigation of the influence of strain levels on the material stiffness. Several tests with various strain rates and temperatures have been conducted to measure to what extent the influence of the strain level changes.

In Figure 9 the tension test set-up for experiments at room temperature is shown. The material sample is placed in between two clamps of which the upper one is used to deform the specimen. An extensometer is attached to the sample that measures the strain. Figure 10 shows the oven that is used to conduct tests at elevated temperatures. The remaining set-up inside the oven is identical to that in Figure 9.

Figure 9: Tension test at room temperature: Clamped specimen with attached extensometer.

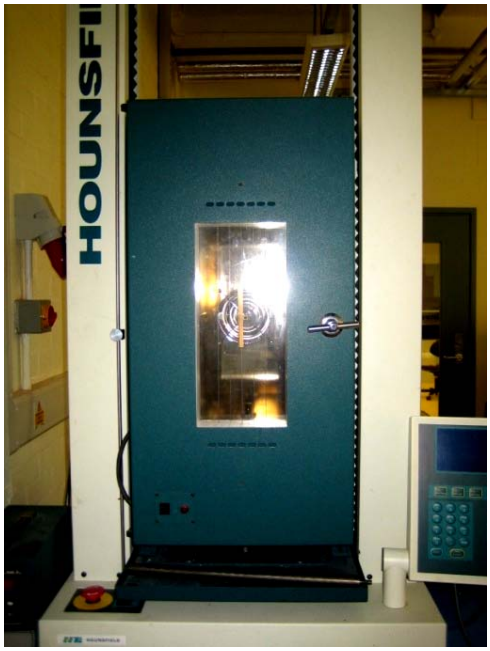

Figure 10: Tension test at elevated temperature: Chamber where specimen is placed in.

3.2 Theory

The tension tests are displacement controlled and have a constant velocity throughout the test. The strain is the extension of the specimen over its original length

$$\varepsilon = \frac{\Delta l}{l} \tag{15}$$

Due to the clamping of the specimen a small force is induced in the beginning of the test. Therefore the E-modulus takes into account the initial stress σ_0

$$E = \frac{\sigma - \sigma_0}{\varepsilon} \tag{16}$$

The theoretical strain rate of the test is the displacement velocity v over the length of the

specimen

$$\dot{\varepsilon} = \frac{v}{l} \tag{17}$$

In practice though, mainly due to compliance of the machine and the visco-elastic effect, the strain rate is not constant. Therefore the strain rate is calculated with the strain and the elapsed time t according to

$$\dot{\varepsilon} = \frac{\varepsilon}{t} \tag{18}$$

In order to obtain the corresponding *tan δ* for a tension test the strain rate has to be converted into the corresponding frequency in the DMTA test. The strain rate is converted to the corresponding DMTA frequency via Eq. 19.

$$f_{DMTA} = 1361.11088 \cdot \dot{\varepsilon}_{Tension} \tag{19}$$

3.3 Conducted Tests and Results

Four different settings have been investigated by means of tension tests. They are listed in Table 1. It shows how many samples have been analyzed, the temperature T and the strain rate ε̇. The latter is converted into the corresponding DMTA frequency according to Eq. 19. The loss tangent *tan δ* is then obtained from the DMTA data by interpolation of temperature and frequency. One setting is characterized by elevated and the rest by room temperature.

	1	***2***	***3***	***4***
number of tests	*4*	*4*	*6*	*6*
T	*23 °C*	*23 °C*	*23 °C*	*56 °C*
$\dot{\varepsilon}_{Tension}$	*2.0E-4 s^{-1}*	*4.25E-5 s^{-1}*	*2.8E-5 s^{-1}*	*3.8E-5 s^{-1}*
f_{DMTA}	*0.272 s^{-1}*	*0.058 s^{-1}*	*0.038 s^{-1}*	*0.052 s^{-1}*
tan δ	*0.12*	*0.15*	*0.16*	*0.25*

Table 1: Four different tension test settings. Number of tests temperature, strain rate, frequency and loss tangent are listed.

Each obtained stress strain curve was fitted by means of polynomials and those corresponding to one setting were averaged.

3.3.1 Investigation of the influence of strain rates

At first the influence of a change of the strain rate on the stress strain curves is investigated. The resulting curves for test settings 1, 2 and 3 are shown in Figure 11. It is clearly observable that tests with a higher strain rate have a higher resistance leading to higher stresses. Their degree of nonlinearity is also higher, which means the degree of the visco-elastic effect increases with increasing strain rate. As explained in Section 2.3 this is not represented in the loss tangent. In case of strain rate the loss tangent is not an indicator on the degree of the visco-elastic effect.

This leads to the development of the E-moduli as shown in Figure 12 with high values at low strain levels for large strain rates decreasing with decreasing strain rate and increasing strain level. At the same time the influence of the strain level decreases with decreasing strain rate.

3.3.2 Investigation of the influence of temperature

After the strain rate now the influence of a change of the temperature on the stress strain relationship is investigated. The curves for test settings 1 and 4 are shown in Figure 13. The two settings do not have identical strain rates but the small difference is negligible.

Note that the curve at elevated temperature starts at the DMTA strain level, because it has been manually shifted to that strain level. This has been done because the heated oven had to be opened in order to place the sample in the device. At that point the temperature drops and hence the specimen shortens. This corresponds to applying a tensile force and thus, because of the elapsed time until the experiment is started, the strain does not start at zero. Therefore the starting strain level was assumed to be the DMTA strain level as the E-modulus at that level approximates that anticipated from the DMTA results (see Section 4.1).

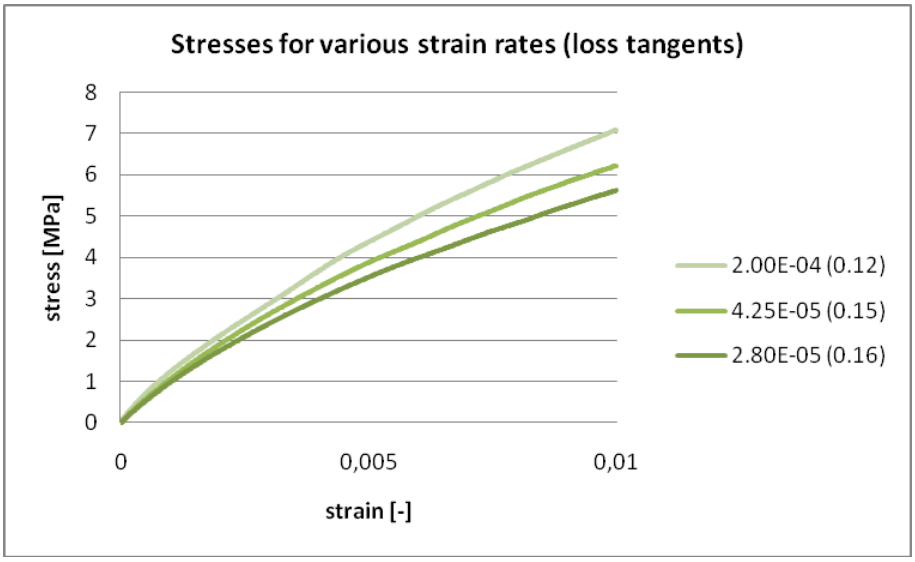

Figure 11: Stress plotted against strain for various strain rates (loss tangents) obtained from tension tests.

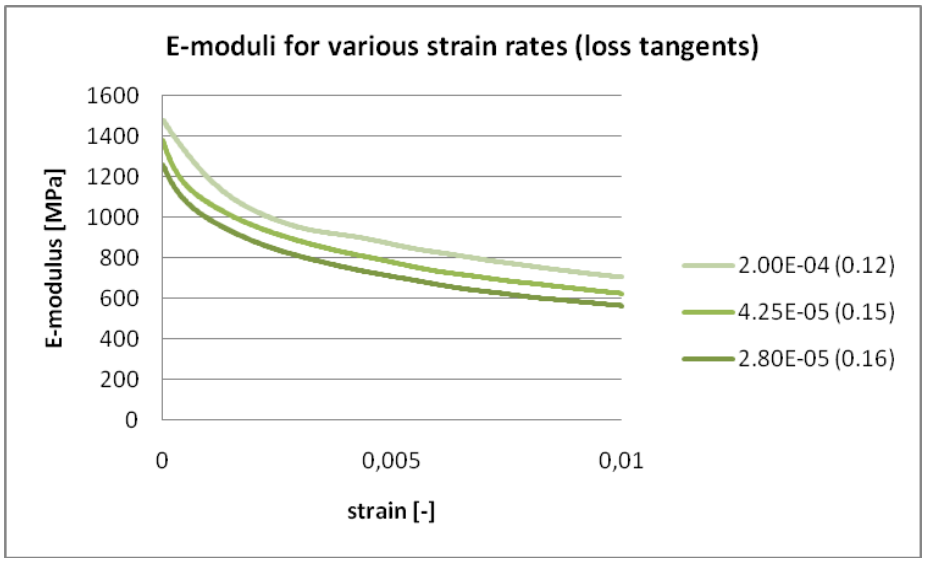

Figure 12: E-modulus plotted against strain for various strain rates (loss tangents) obtained from tension tests.

It is clearly observable that the test at room temperature has a higher resistance and leads to higher stresses. The nonlinearity of the curve at elevated temperature is hardly visible, what might lead to the conclusion that the visco-elastic effect would decrease with increasing temperature and loss tangent. Consideration of the development of the E-moduli as shown in Figure 14 though shows that the curve is in fact highly nonlinear for a small strain interval and only becomes linear after a certain strain level. Furthermore the reduction of the E-modulus is even higher than for lower loss tangents, since the ratio between the E-modulus at the DMTA strain level and that at 1% strain equals to 2. For the test at elevated temperature this value equals to 2.5. Hence it can be concluded that with increasing loss tangent the decrease of material stiffness occurs in a smaller strain interval and is greater than for lower loss tangents.

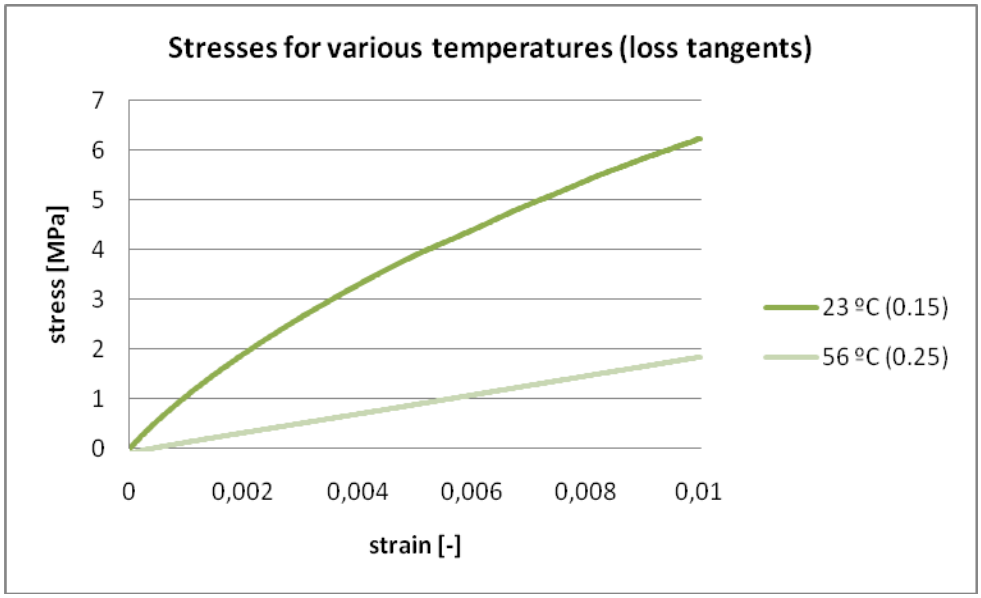

Figure 13: Stress plotted against strain for various temperatures (loss tangents) obtained from tension tests.

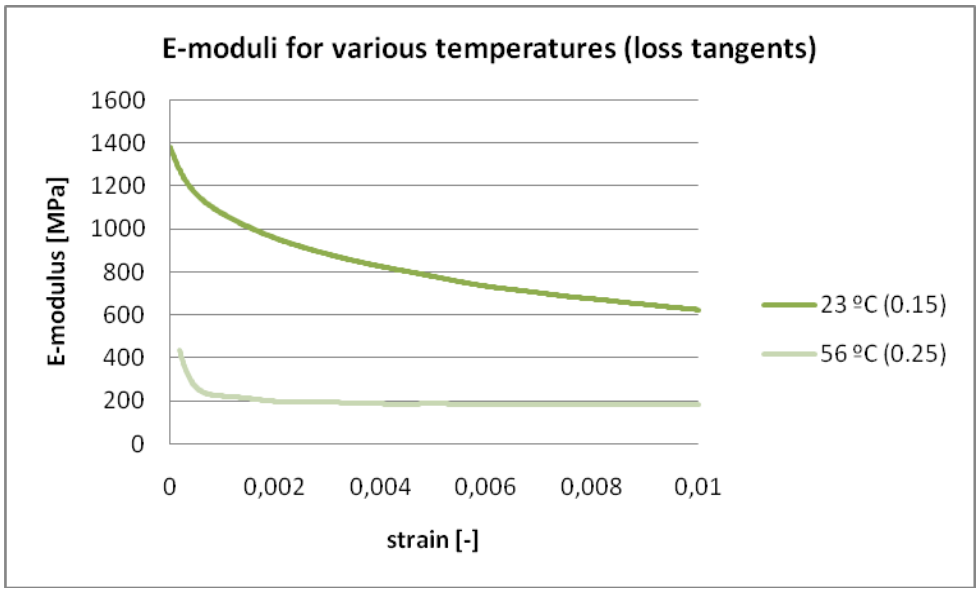

Figure 14: E-modulus plotted against strain for various temperatures (loss tangents) obtained from tension tests.

4 APPLICATION IN NUMERICAL MODELING

4.1 Theory

The combination of the results obtained from the DMTA tests and the tension tests yields a secant modulus that takes temperature, strain rate and strain level as well as their interrelation into account. This modulus will be called E_{FE} as it will be used within the Finite Element method. The starting point to define that value is the storage modulus *E'* obtained from the DMTA test. For the FE model naturally the total E-modulus is required and not the elastic part of it. Therefore, according to Eq. 12, this elastic part has to be multiplied by *(1+tan δ)*, called fac_{visco} from here forth, to obtain the total E-modulus which is the sum of the elastic and the inelastic part

$$E = E' + E'' = E' \cdot (1 + tan\,\delta) = E' \cdot fac_{visco} \tag{20}$$

The proof that the total E-modulus obtained by Eq. 20 is in fact the real E-modulus can be furnished by comparing it to the E-modulus obtained from the tension tests at the DMTA strain level according to Eq. 13. This was done for the four tension test settings. The results are listed in Table 2.

	1	***2***	***3***	***4***
T [°C]	*23*	*23*	*23*	*56*
$\dot{\varepsilon}_{Tension}$ ***[s^{-1}]***	*2.0E-4*	*4.25E-5*	*2.8E-5*	*3.8E-5*
f_{DMTA} ***[s^{-1}]***	*0.272*	*0.058*	*0.038*	*0.052*
tan δ [-]	*0.12*	*0.15*	*0.16*	*0.25*
E' [MPa]	*1289*	*1106*	*1073*	*375*
$E' \cdot fac_{visco}$ ***[MPa]***	*1442*	*1278*	*1247*	*470*
$E_{Tension}(\varepsilon_{DMTA})$ ***[MPa]***	*1420*	*1274*	*1177*	*436*

Table 2: Comparison of the total E-modulus obtained from DMTA tests with the E-modulus at the DMTA strain level from the tension tests. The total E-modulus is obtained by multiplying *E'* by fac_{visco}.

The total E-modulus from the DMTA test and the one from the tension tests differ by at most 7 %.

The results from the tension tests are now exploited in order to take the strain level into account. Therefore another factor fac_{level} is introduced.

$$fac_{level} = \frac{E_{Tension}(\varepsilon_{Pipe})}{E_{Tension}(\varepsilon_{DMTA})} \tag{21}$$

It will be used to reduce the E-modulus obtained from the DMTA tests according to a representative strain level. At first fac_{level} will be discussed for the different strain rates. The corresponding curves are illustrated in Figure 15. One can see that the variation between the curves and the loss tangent is rather small. Thus, the influence of strain rate on fac_{level} will be neglected.

Now the influence of varying temperatures on fac_{level} will be discussed. The corresponding curves are illustrated in Figure 16. One can see that the influence of the temperature is more significant than the strain rate. Not only is the quantitative difference more significant but also the shape of the curves changes. Therefore the influence of the temperature on the strain level will be considered. The degree of the visco-elastic effect is measured by means of *tan δ*. For a

tan δ=0 the material behaviour is purely elastic, thus the E-modulus is constant in that case. The theoretical curve for that case has been added in Figure 16. To obtain a fac_{level} for any other temperature, the values are interpolated by means of the actual loss tangent.

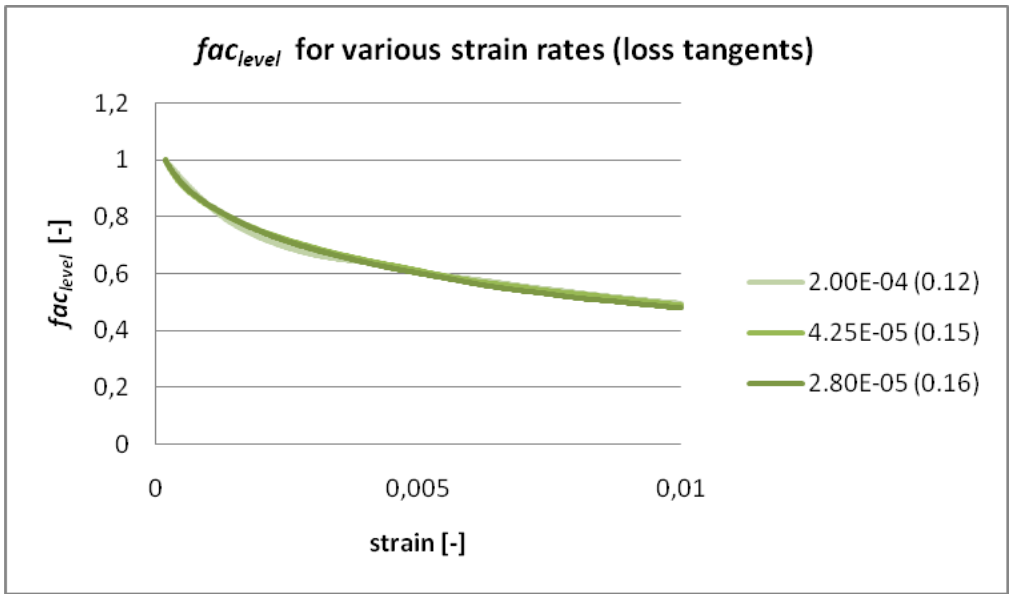

Figure 15: fac_{level} plotted against strain for various strain rates (loss tangents) obtained from tension tests.

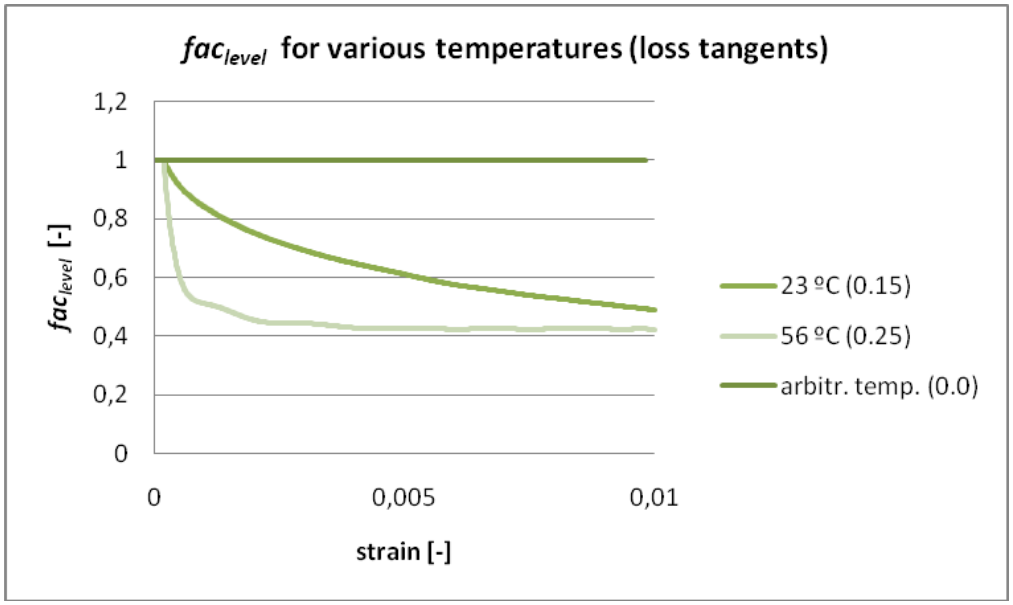

Figure 16: fac_{level} plotted against strain for various temperatures (loss tangents) obtained from tension tests.

With the two correction factors the final E-modulus for the FE analyses reads:

$$E_{FE} = E' \cdot fac_{visco} \cdot fac_{level} \tag{22}$$

In order to evaluate Eq. 22 ε_{Pipe}, $\dot{\varepsilon}_{Pipe}$ and T_{Pipe} have to be available. As mentioned before for a pipe stored in constant temperature for a sufficiently long time the pipe temperature can be assumed to be stationary across its volume. For the strain level and strain rate though a

representative value has to be found. In case of the strain level this is taken to be 80% of the maximum principle strains found by FE analyses.

$$\varepsilon_{Pipe} = 0.8 \cdot \varepsilon_1^{max} \tag{23}$$

The representative strain rate is the representative strain level divided by the duration of the stiffness test t_{test}.

$$\dot{\varepsilon}_{Pipe} = \frac{\varepsilon_{Pipe}}{t_{test}} \tag{24}$$

Eq. 22 has been evaluated for a temperature range 5°C to 49°C and a strain rate range from 2E-5 s^{-1} to 1E-4 s^{-1}. The results are plotted in Figure 17. The strain level at which fac_{visco} has been evaluated was set to 4E-3.

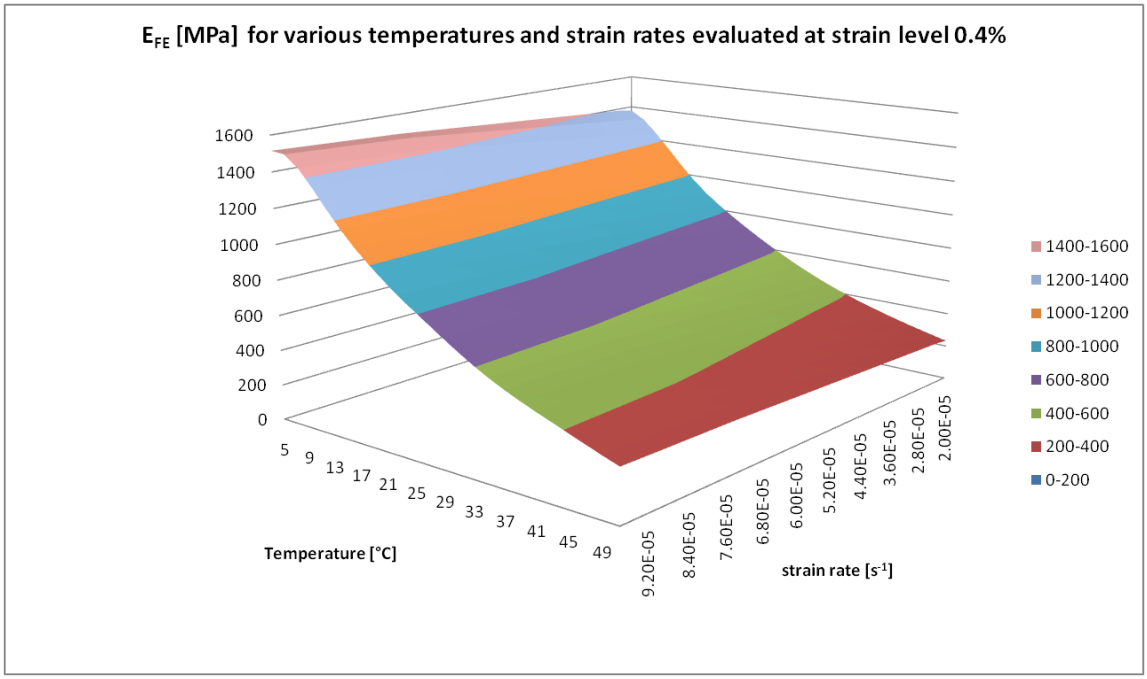

Figure 17: E_{FE} plotted against temperature and various strain rates.

4.2 Finite Element Model

The FE model solved in this context simulates the Ringstiffness test. In this test, a pipe sample is placed in between two parallel horizontal plates and compressed up to a vertical deflection equal to 3% of the pipe's inner diameter. The machine monitors the force F that is necessary to move the top plate with constant velocity, which in return yields the ringstiffness SN with

$$SN = \frac{F \cdot \left(0.0186 + 0.025 \cdot \frac{y}{D}\right)}{y \cdot L} \tag{25}$$

Here, y is the vertical deflection, L is the length of the pipe sample, and D is the inner diameter. Due to symmetry of the pipe and the loading only one eighth of the pipe is modeled.

The mesh contains linear shell elements and the plate loading is idealized by an enforced displacement of the nodes at the pipe crown.

4.3 Application to Pipe Experiments

The derived equations are now exploited in order to simulate the Ringstiffness test and compare the results to actual experiments. Experiments with four different pipes are available. The results from the experiments and the FE analyses are compared in Table 3. The FE simulations differ from the experiments by at most 7 %. Considering the assumptions involved in the simulation these results can be called sufficiently accurate.

5 CONCLUSIONS

The objective of the present work was to investigate the influence of temperature, strain rate and strain level on the material stiffness of HDPE that is used for the production of structured-wall pipes. With this knowledge a more accurate numerical simulation was aimed for while using a linear material model to maximize the efficiency.

To this end several material tests of two different types have been conducted, DMTA tests and tension tests. The former was used to investigate the influence of temperature and strain rate and the latter to investigate the influence of strain levels. A formula has been developed that combines the obtained data and converts it into the E-modulus to be used for the FE analysis. The results of several real pipe experiments were compared to those of the FE analyses. The obtained results are sufficiently accurate within the scope of the work.

temperature	[°C]	23	23	23	23
sample length	[mm]	567.7	585.8	561.1	448.4
diameter	[mm]	2225	1601	1007	598
pipe deformation	[mm]	66.8	48.0	30.2	17.9
deformation speed	[mm/min]	50	50	50	20
experiment duration	[s]	80.2	57.6	36.2	53.7
ε_{Pipe}	[-]	3.87E-03	5.33E-03	5.08E-03	5.47E-03
$\dot{\varepsilon}_{Pipe}$	[s^{-1}]	4.83E-04	9.25E-05	1.4E-04	1.01E-04
f	[s^{-1}]	0.66	0.13	0.19	0.14
E'	[MPa]	1119.1	1193	1235.7	1201.2
$tan\ \delta$	[-]	0.1526	0.1376	0.1293	0.136
fac_{visco}	[-]	1.1526	1.1376	1.1293	1.136
fac_{level}	[-]	0.6649	0.652	0.6798	0.6521
E_{FE}	[MPa]	857.6	884.8	948.4	889.7
Ringstiffness Simulation	[kN/m²]	2.1	7.4	7.4	8.1
Ringstiffness Experiment	[kN/m²]	2.2	7.3	6.9	8.1

Table 3: Specifications for four experiments and comparison with the results obtained from FE analyses.

REFERENCES

Bilgin, Ö., Stewart, H., O'Rourke, T., Thermal and Mechanical Properties of Polyethylene Pipes, *Journal of Materials in Civil Engineering*, 19:1043-1052, 2007.

British Standards Institution, Plastics piping and ducting systems – Thermoplastics pipes – Determination of ring flexibility, BS EN 1446 : 1996, British Standards Institution, London,

1996.
Hall, C., *Polymer Material – An Introduction for Technologists and Scientists*, Macmillan Education Ltd, London, 1989.
Ferry, J., *Viscoelastic Properties of Polymers*, John Wiley and Sons, New York, 1980.
Love, C., Xian, G., Karbhari, V. Thermal, Mechanical and Adhesive Properties of HDPE/ Reactive Ethylene Terpolymer Blends, *Journal of Applied Polymer Science*, 104:331–338, 2005.
Moore, I., Zhang, C., Nonlinear Predictions for HDPE Pipe Response under Parallel Plate Loading, *Journal of Transportation Engineering*, 124:286-292, 1998.
Sha, H., Zhang, X., Harrison, I., A Dynamic Mechanical Thermal Analysis (DMTA) Study of Polyethylenes, *Thermochimica Acta*, 192:233-242, 1991.